Finite element simulation of a 3D woven fabric: determination of the initial configuration and characterization of the mechanical behavior

Yanneck Wielhorski, Damien Durville

Finite element simulation of a 3D woven fabric: determination of the initial configuration and characterization of the mechanical behavior.

Conference Paper · May 2015

CITATION
1

READS
237

2 authors:

Yanneck Wielhorski
SAFRAN GROUP
19 PUBLICATIONS **61** CITATIONS
SEE PROFILE

Damien Durville
CentraleSupélec
73 PUBLICATIONS **714** CITATIONS
SEE PROFILE

FINITE ELEMENT SIMULATION OF A 3D WOVEN FABRIC: DETERMINATION OF THE INITIAL CONFIGURATION AND CHARACTERIZATION OF THE MECHANICAL BEHAVIOR

Wielhorski Y.[1], Durville D.[2]*

[1]*Snecma/Safran, Villaroche, Réau, France*

[2]*LMSSMat, CNRS UMR 8578 - Ecole Centrale Paris, Châtenay Malabry, France*

*corresponding author: *damien.durville@snecma.fr*

ABSTRACT

At the mesoscale, the modelling of the fabric lies in an assembly of interlacing yarns or tows, which are considered as a continuous media, and can give information on the pore scale between the bundles. However, a thinner scale can be useful to reach more accurate mechanical properties and geometrical description. The proposed methodology allows to reach the microscale, the constitutive fiber scale, for the simulation of different types of entangled materials. To determine the unknown initial configuration, we start from a flat and highly inter-penetrated configuration, tows from different layers, represented by bundles of so-called macro-filaments, are gradually separated by using contact interactions to reduce the initial gaps, until reaching an equilibrium configuration, which fulfills contact conditions, and matches the stacking order prescribed by the selected weaving pattern. By this means, tow trajectories and variations of cross-section shapes along the tows can be obtained, only defining the structure of tows and the weaving pattern. Unit cells involving up to tens of tows can be considered by this approach, using about twenty macro-filaments per tow. Comparisons of the initial geometry obtained by simulation with tomography data will be presented. Once the initial configuration has been computed, various loading cases can be simulated in order to identify the mechanical behavior of 3D woven fabric, by prescribing displacements on the borders of the samples studied, of by deforming these samples by means of moving rigid tools. Results of transverse compression simulations will be presented and compared to experimental data.

THEORETICAL MODEL

1. PRINCIPLES

The mechanical equilibrium of assemblies of fibres constituting the studied textile materials is formulated in the form of the following principle of virtual work:

Find u kinematically admissible such that $\forall v$ kinematically admissible:

$$\sum_{i=1,N}\left(W_{\text{int}}^{i}(u,v) + \sum_{j=I,N} W_{cf}^{ij}(u,v) \right) = \sum_{i=1,N} W_{ext}^{i}(v) \qquad \text{(Eq. 1)}$$

where W_{int}^{i} stands for the internal virtual work of each individual fibre, and W_{cf}^{ij} stands for the virtual work of contact-friction interactions between fibres *i* and *j*.

2. ENRICHED KINEMATICAL BEAM MODEL

The fibres are represented by an enriched kinematical beam model based on a first order Taylor expansion of the placement of any particle belonging to the beam with respect to its transversal coordinates. The position of each material particle ξ is defined by its curvilinear abscissa ξ_3 and its coordinates (ξ_1,ξ_2) relative to the cross section of the beam (*Figure 1*). By defining, x_0 the position of the centre of the beam cross-section and g_α its director vectors, the placement of the particle ξ at time t is given by:

$$x(\xi,t) = x_0(\xi_3,t) + \xi_\alpha g_\alpha(\xi_3,t), (\alpha = 1,2) \qquad \text{(Eq. 2)}$$

Note that the motion of cross-sections is entirely described by three vector fields and nine degrees of freedom. This kinematical model allows deformation of cross-sections to be taken into account and 3D constitutive laws to be used.

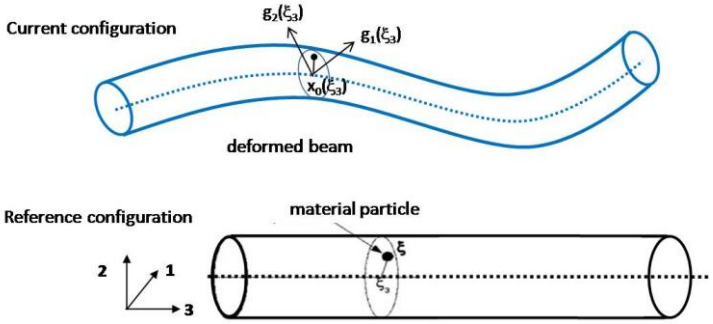

Figure 1: Straight and deformed beam and representation of the three kinematical vectors used to define the position of a material particle in the kinematical beam model

3. CONTACT AND FRICTION MODELLING

To localize contact interactions, zones of proximity are first defined by pairs of parts of beam centroidal lines which are close enough. Then, an intermediate geometry is defined for each zone of proximity, as the average between the both parts constituting the zone of proximity, in order to approximate the unknown actual contact zone. Contact is then defined with respect to these intermediate geometries, by creating contact elements at discrete locations on this intermediate geometry. A contact element, denoted $E_c^{ij}(x_c)$, is defined as a pair of particles (ξ_c^i, ξ_c^j), belonging respectively to the beams *i* and *j*, which are predicted to enter into contact at the location x_c. Defining contact with respect to the intermediate geometry leads to a symmetrical treatment of both interacting beams, unlike usual master-slave strategies. The determination process of contact depends on the displacement solution and needs therefore to be iterated within each loading step.

To control the interpenetration between beams, a gap function is defined for each contact element as the distance between the two particles of the contact element measured according to a normal contact direction:

$$gap\left(E_c^{ij}(x_c)\right) = \left(x^i(\xi_c^i) - x^j(\xi_c^j), N(x_c)\right) \qquad \text{(Eq. 3)}$$

The contact-friction interaction force $\mathbf{R}_{cf}^{ij}(\mathbf{x_c})$ is splitted for each contact element into a normal component (R_N^{ij}) and a tangential part ($\mathbf{R}_T^{ij}$) depending on:

$$R_{cf}^{ij}(x_c) = R_N^{ij}(x_c) N_c^{ij}(x_c) + R_T^{ij}(x_c) \qquad \text{(Eq. 4)}$$

Note that linearized kinematical contact conditions, expressed for each contact element, can be formulated such as the gap function has to remain positive. A regularized and adaptative penalty method is used to express the normal reaction as function of the gap. The quadratic regularization of the penalty for very low penetrations, and a local adjustment of the penalty coefficient, for each zone of proximity so as to control a maximum allowed penetration, are used to smooth the transition between contacting and non-contacting phases. As far tangential components are concerned, a regularized Coulomb's law including a small reversible elastic displacement before sliding is used to express the friction.

4. GRADUAL SEPARATION PRINCIPLE FOR THE DETERMINATION OF THE INITIAL CONFIGURATION

As the trajectories of each yarn in the initial configuration cannot be predicted a priori, we start from an arbitrary configuration (*Figure 4a*), where all yarns are straight and lie in the same plane, inter-penetrating each other. The selected weaving pattern prescribes, at each crossing between two yarns, which should be above or below the other, thus defining a stacking order. This stacking order is simply defined by a low triangular matrix, whose values may be +1, -1, or 0, depending on whether the first yarn should be above, below, or in undefined position with respect to the second yarn. Both yarns may have two different weaving orientations (weft or warp), or may have the same orientation and correspond to different layers (see *Figure 2*). Knowing this stacking order, the principle for the gradual separation is to let contact-friction interactions move intersecting fibres away from each other until reaching a mechanically equilibrated configuration, which fulfills the weaving pattern. Due to very large initial penetrations, using the standard contact algorithm would induce large instabilities and prevent convergence. Two ingredients are necessary for the proposed gradual separation. First, the normal contact direction used to define the gap needs to be oriented in the right direction in order fibres to be moved according to the stacking order. Second, since penetrations may be very large, and therefore may prevent the convergence of contact algorithm, the gaps are reduced little by little at each loading increment. During this initial stage, a gap reduction factor g_{red} is defined as a fraction of a typical diameter of fibre. When the absolute value of the penetration at a contact element is larger than the threshold g_{red}, the latter value is considered for the computation of the normal reaction in order not to limit the order of magnitude of these reactions.

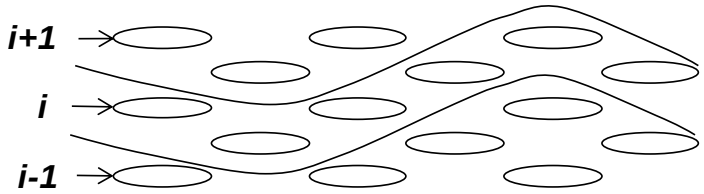

Figure 2: Example of pattern of warp plane of a theoretical 3D fabric

5. BOUNDARY CONDITIONS

In the case of the multi-scale structure of 3D woven fabrics, displacements (translations and rotations) need to be controlled not only at ends of fibres, but also at ends of higher level components, namely tows, columns of tows, and warp and weft layers. For this purpose, a hierarchical control of boundary conditions is proposed. Rigid bodies are introduced and attached at ends of components of different levels (tows, columns and layers). Displacements at ends of a set of subcomponents from a given higher level component are then prescribed with respect to the local frame defined by the rigid body attached to this higher level

component. In order to allow ends of subcomponents the possibility to move and rearrange, average conditions can be defined. Boundary conditions applied to the unit cell considered, which are formulated using this hierarchical structure of rigid bodies, are chosen periodic.

NUMERICAL RESULTS

1. DESCRIPTION OF THE SIMULATED 3D WOVEN FABRIC

Currently, in industrial cases, the large number of fibres composing a tow (typically several tens of thousands), and then the whole sample, does not allow us to simulate all of the fibres. Therefore, to get around this issue, we represent each bundle made of a given number of actual fibres, denoted n_{micro}, by an equivalent "macro-fibre", whose tensile and bending stiffnesses are evaluated as the sums of corresponding stiffnesses of the actual fibres constituting the "macro-fibre". To determine the value of their radius, the idea is to keep the overall cross-section of microfibres inside a tow as constant and equal to the overall cross-section of the macrofibres. The radius of the macrofibres R_{macro} is then given by the following relation:

$$R_{macro} = \sqrt{\frac{n_{micro}}{N_{macro}}} r_{micro} \qquad \text{(Eq. 5)}$$

The sample simulated here is based on a 3D woven fabric with 64 yarns divided into 8 warp planes and 8 weft planes. The yarns are distributed as follows: 32 tows in the weft direction and 32 yarns in the warp direction. In the example showed hereinafter, 37 macrofibres are considered per yarn, leading to a total number of 2,368 macrofibres. The main features of this 3D fabric are summarized in *Table 1*.

Table 1: Few characteristics of the simulated 3D fabric

Characteristics	Sub category	Weft	Warp
Geometry	Number of macrofibres N_{macro} per tow	37	
	Total number of macrofibres	2,368	
	Average radius of microfibres r_{micro} (µm)	2.5	
	Radius of the macrofibres R_{macro} (µm)	126	
	Number of tows	32	32
	Number of columns	8	8
Mechanical properties of fibres	Longitudinal Young's modulus (MPa)	276,000	
	Poisson's ratio	0.26	

2. TWISTING STEP

In fact, to maintain the cohesion of yarns, each one endures beforehand a twisting of around 20 turns per metre. A preliminary step is devoted to the twisting of each yarn to be close to the actual experimental conditions. Here a twisting angle of 120° is applied in six increments.

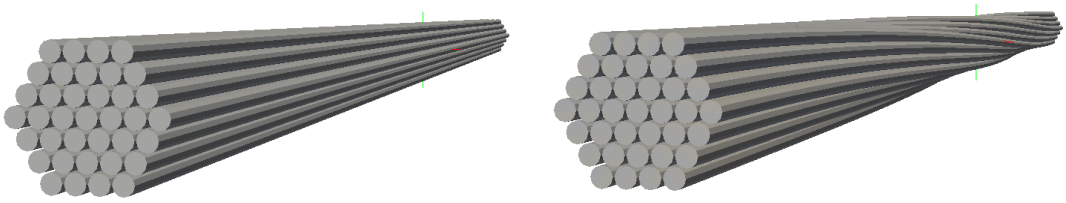

Figure 3: Evolution of the twisting step for a tow from the initial step to a twisting of 120°

3. COMPUTATION OF THE INITIAL CONFIGURATION

First, we define an inter-penetrated configuration (Figure 4a) where all the yarns belonging to the same column occupy the same position. This first configuration is only defined by the length of the sample in warp and weft directions and the distribution of tows in each column. At the end of the computation of the initial configuration, after the procedure of gradual separation of yarns, the initial configuration is obtained as an equilibrium configuration (Figure 4b). Some numerical details of computation are given *Table 2*.

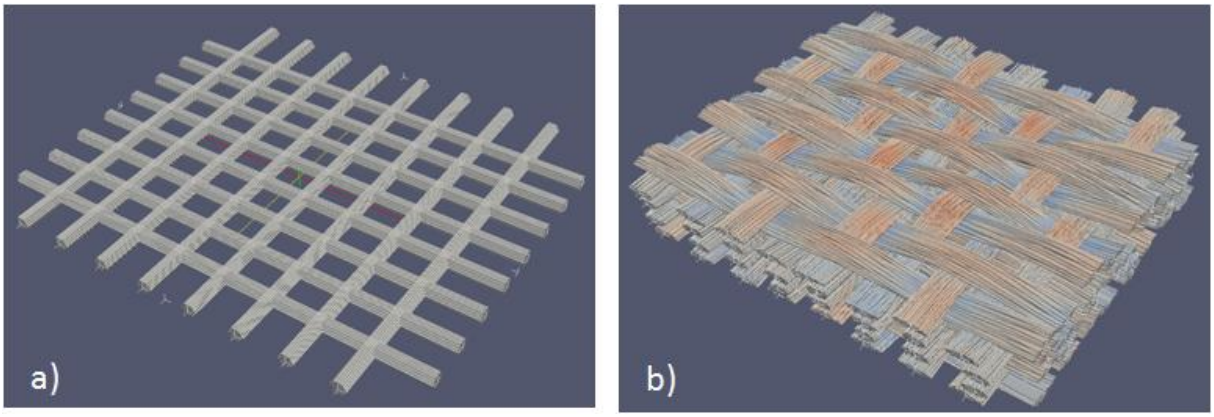

Figure 4: a) Interpenetrated configuration (starting state); b) Equilibrium configuration (initial state)

Table 2: Numerical characteristics of the studied case

Characteristics	Sub category	
FE discretization	No. of FE	71,040
	No. of dofs	1,300,032
Contact	No. of contact elements	from ~ 500,000 to 1,400,000

4. COMPUTATION OF THE COMPRESSION

After the initial configuration of the 3D woven fabric is obtained, many kinds of mechanical loads can then be applied. Here, we show a simulation of a transverse compression test between two plates that we have performed from the computed initial configuration. Figure 5 represents the final stage of the transverse compression corresponding to the target Fiber Volume Fraction.

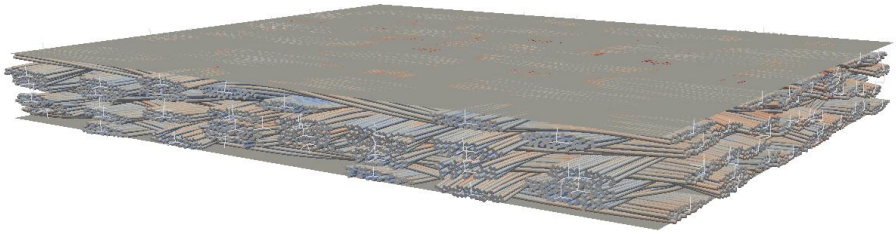

Figure 5: Final step of the compaction at the target Fiber Volume Fraction

An algorithm based a Delaunay triangulation has been performed to extract the shape of each tow. Actually, each tow can be described by defining the number of cross planes and each of them is described by a number of points. Figure 6 shows the shape of one tow with 30 cross sections and 200 points by cross-section.

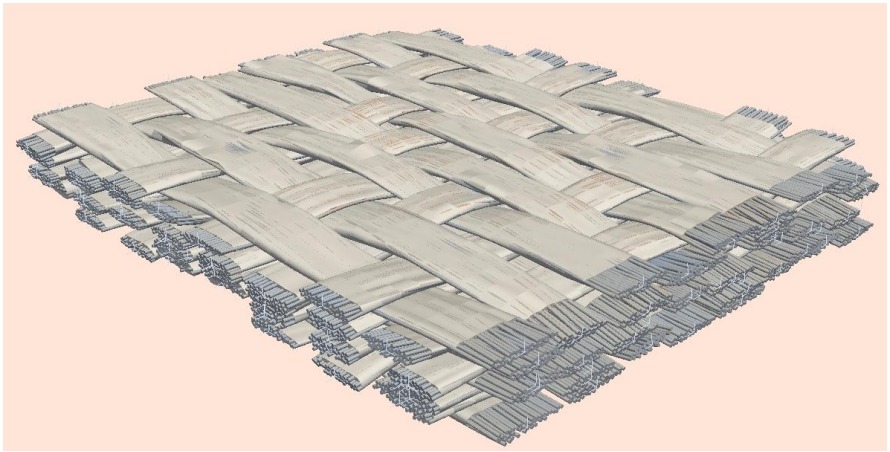

Figure 6: Superposition of macrofibres and the tow shapes

During the transverse compression simulation, the macrofibres inside the tows endure a rearrangement. Figure 7 shows this rearrangement at a tip of a tow at three different compaction steps.

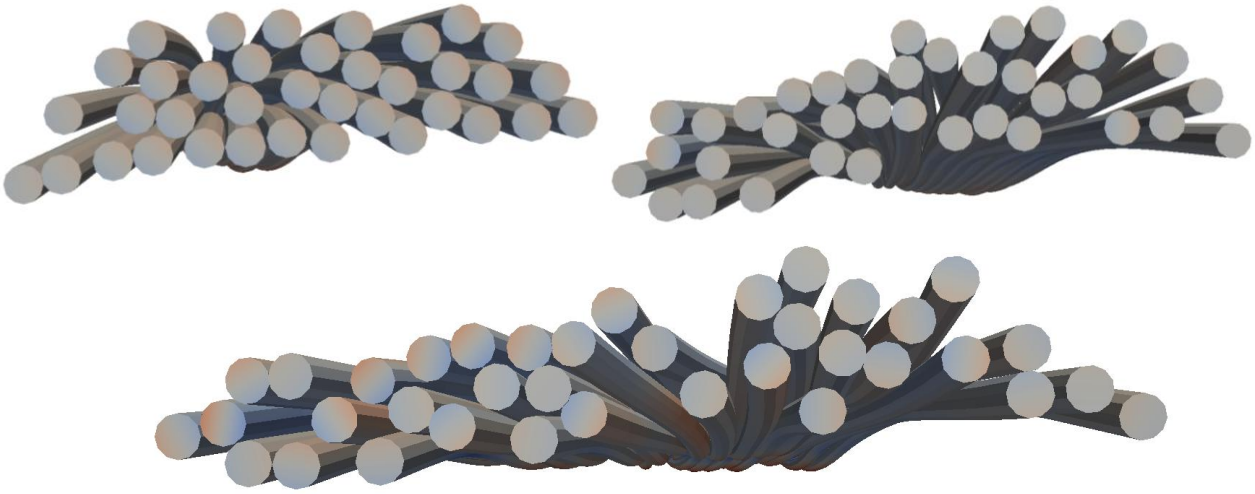

Figure 7: Rearrangement of macrofibres during the compaction

Figure 8 shows normalized compaction curves representing the evolution of the thickness of the 3D fabric as a function of the strength applied by the plates. The curve with blue circle markers represents the numerical results from Multifil and the others represent experimental data from three different samples. Here our simulation is performed with 37 macrofibers, a tension of 10dN at one tip of yarns as well as for the warp and weft yarns. Furthermore, we set the step of the compression plate at 50µm. So we can observe a discrepancy of the results from the numerical simulation with the experimental data. This is maybe due to the isotropic mechanical behaviour of the macrofibers.

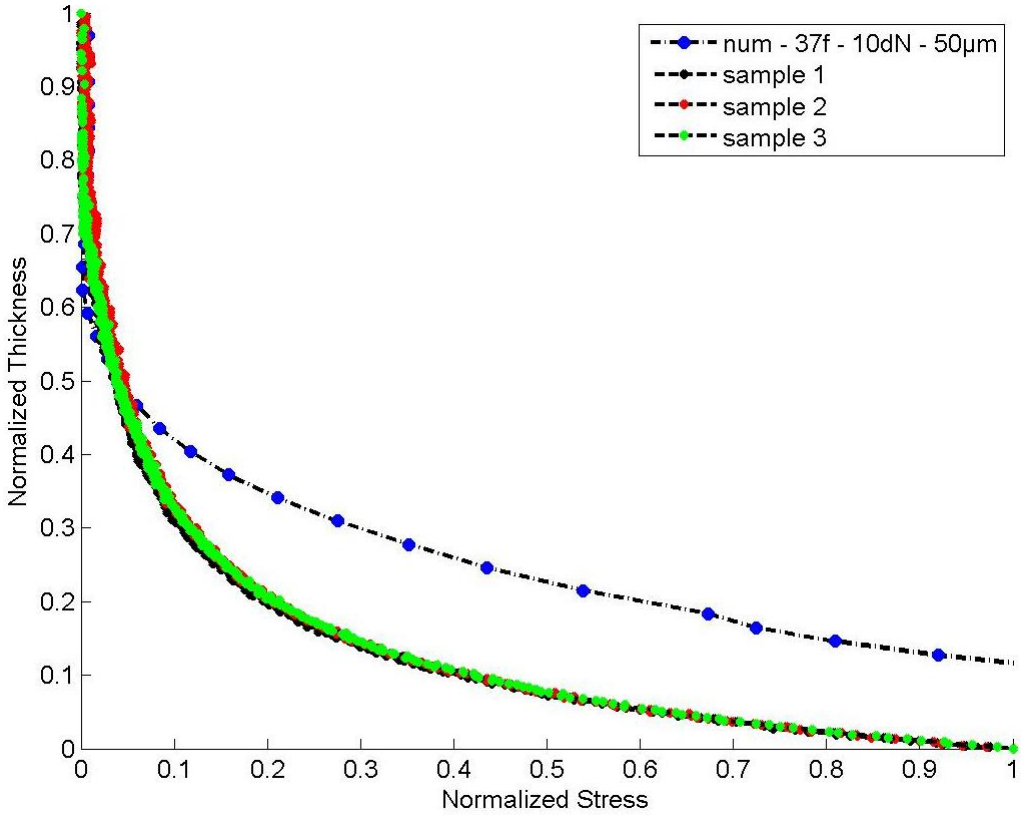

Figure 8: Compaction curves: experimental transverse compression tests for different samples (blue, red and green diamond markers) and the numerical transverse compression test (red dot marker)

CONCLUSION

A method based on the detection and modelling of the contact-friction interactions between fibres, represented by a finite strain beam model, is used to determine the initial configuration of a 3D fabric as a mechanical equilibrium and a compacted state corresponding to a target fibre volume fraction. As the proposed method allows the rearrangement of the components of different levels (fibres, tows and columns), valuable information about the geometry of these components (trajectories of fibres and tows, shapes of the cross-sections, void distributions within the fabric) can be retrieved from the simulations. The model can be moreover used to determine the response of the 3D fabric to various loading cases in order to identify its mechanical properties.

One of the nearest improvements is to set the orthotropic young modulus of the macrofibers. Besides, some geometrical comparisons should be done in the future in addition to mechanical validations.

ACKNOWLEGDEMENTS

The collaboration with *Snecma* is gratefully acknowledged. This work was supported under the PRC Composites, French research project funded by DGAC, involving SAFRAN Group, ONERA and CNRS.

REFERENCES

1. Lomov, S.V., Gusakov, A.V., Huysmans, G., Prodromou, A., Verpoest, I. Textile geometry preprocessor for meso-mechanical models of woven composites. Composite Science and Technology, 60: 2083–2095, 2000

2. Lin, H., Zeng, X., Sherburn, M., Long, A.C., Clifford, M.J. Automated geometric modelling of textile structures. Textile Research Journal, 82: 1689–1702, 2012

3. Miao, Y., Zhou, E., Wang, Y., Cheeseman, B.A. Mechanics of textile composites: Micro-geometry. Composite Science and Technology, 68: 1671–1678, 2008

4. Charmetant, A., Orliac, J. G., Vidal-Salle, E., Boisse, P., Hyperelastic model for large deformation analysis of 3D interlock composite preforms, Composite Science and Technology, 72: 1352-1360, 2012

5. Vilfayeau, J., Crépin, D., Boussu, F., Soulat, D., Boisse, P. Numerical modelling of the weaving process for textile composite. Key Engineering Materials, 554-557: 472–477, 2013

6. Durville, D. Simulation of the mechanical behaviour of woven fabrics at the scale of fibers. International Journal of Material Forming, 3: S1241–S1251, 2010

7. Durville, D. Contact-friction modelling within elastic beam assemblies: an application to knot tightening. Computational Mechanics, 49: 687–707, 2012